Various Approaches to Torque Calculations by FEM and BEM

Mladen TRLEP, Anton HAMLER, Božidar HRIBERNIK

University of Maribor, Faculty of Electrical Engineering and Computer Science
Smetanova ul. 17, 2000 Maribor, Slovenia

Abstract - Different algorithms for the torque calculation by Maxwell stress method (MSM) are dealt with in the paper. The aim of designing these algorithms was to reduce the influence of the choice of the integration path and discretization of the air gap between the stator and rotor on the accuracy of the results. In some of these algorithms the connection between the stator and rotor is released. For the magnetic field calculation the finite element method (FEM), boundary element method (BEM), and hybrid finite element - boundary element method (HM) were used. The calculation results were tested on a permanent magnet DC motor and a single phase brushless motor.

I. Introduction

Torque is one of the basic parameters of each motor. For the torque calculation different methods exist. Recently, the most frequently used methods have been those where the torque is calculated directly from the magnetic field solution in the motor. The accuracy of these methods depends to a great extent on the accuracy of the magnetic field calculation. The influence of the error of the magnetic field calculation on the torque calculation depends also on the calculation procedure, i.e. on the applied method. For this purpose three basic methods are mainly used: the virtual work method, Maxwell stress method, and magnetizing current method.

The MSM is frequently used in practice due to its simplicity and good results. It enables the calculation of the total torque acting on the rotor or its space distribution around the rotor. The method has also some weaknesses. The results namely depend on the choice of the integration path in the element and on the shape of elements over which the integration path runs. The mentioned drawbacks can be reduced in several ways. Some of them are: the use of higher order elements, mesh refinement in the space between the rotor and stator, adaptation of discretization elements and use of different interpolations of magnetic quantities in the space between the stator and rotor.

The requirements in designing the algorithms were the following: to use the automatic discretization [9] by the first order element, to obtain a good result with a relatively coarse discretization, and that the rotor position is not determined with discretization.

II. The Torque Calculation by the MSM

In the MSM the torque is calculated on the basis of the magnetic field distribution on the closed surface in the air gap around the rotor (1).

$$T = \oint_S \left[\frac{1}{\mu_0} (\boldsymbol{r} \times \boldsymbol{B})(\boldsymbol{B} \cdot \boldsymbol{n}) - \frac{1}{2\mu_0} B^2 (\boldsymbol{r} \times \boldsymbol{n}) \right] \mathrm{d}\boldsymbol{S} \quad (1)$$

where:

- $\boldsymbol{B}$ -vector of magnetic flux density,
- $\boldsymbol{r}$ -radius from the rotation axis to the integration surface S,
- $\boldsymbol{n}$ -unit vector normal to the integration surface,
- μ_0 -permeability of vacuum,
- B -absolute value of magnetic flux density.

In the numerical calculation the integral becomes a sum. For the 2D torque calculation the equation has the following form:

$$T = \frac{L r}{\mu_0} \sum_{e=1}^{Nl_e} B_{ne} B_{te} l_e \quad (2)$$

where:

- B_{ne}, B_{te} -normal and tangential components of $\boldsymbol{B}$ on l_e ,
- l_e -eth part of the integration path,
- L -axial length of the rotor,
- Nl_e -the number of parts on the integration path.

III. Algorithms

In such calculation the accuracy can be increased by increasing Nl_e and the accuracy of B_{ne}, B_{te} in the summations (2). For this purpose four algorithms were developed.

Algorithm A

The magnetic field is calculated by FEM [1]. In the field calculation, first order discretization elements are used. In elements the magnetic density is constant and therefore it is reasonable that each element over which the integration path runs represents one component in sum (2). In this equation index e represents the contribution of the element e. The accuracy of the calculation of the element contribution is influenced by the shape of the element and position of the integration path in it. In the used element the tangential components are discontinuous on the edges of the element. The more the discretization elements resemble the equilateral triangles, the smaller the influence of the discontinuity. For the first order element it is also characteristic that the calculated value of the magnetic density (3) is the most accurate in the center of gravity. It is therefore favorable to choose the integration path in such a way that it runs through the center of gravity of the element.

$$\left.\begin{aligned} B_x &= \frac{\partial}{\partial y}\left(\sum_{i=1}^{3} A_i N_i(x,y)\right) \\ B_y &= -\frac{\partial}{\partial x}\left(\sum_{i=1}^{3} A_i N_i(x,y)\right) \end{aligned}\right\} \Rightarrow B_n, B_t \quad (3)$$

where:

N_i - shape function of the finite element,

A_i - nodal values z components of magnetic vector potentials.

Algorithm B

The magnetic field is calculated by FEM in the same way as in the foregoing case. Afterwards the air gap region between the rotor and stator is extracted and in this region the interpolation of the magnetic vector potential by using Bernstein-Bezier's surfaces is carried out [4], [5]. A complete interpolation surface will be composed of small triangular patches that are smoothly connected (C^1 continuity) at every vertex and along all edges of the finite element mesh. As an interpolation surface over given vertices of the triangular mesh, we use a surface compounded from triangular Bernstein-Bezier's patches of the 3rd order (4).

$$A(r,s,t) = r^3 A_{3,0,0} + s^3 A_{0,3,0} + t^3 A_{0,0,3} + 6rst A_{1,1,1} + 3(r^2 s A_{2,1,0} + rs^2 A_{1,2,0} + s^2 t A_{0,2,1} + st^2 A_{0,1,2} + rt^2 A_{1,0,2} + r^2 t A_{2,0,1}) \quad (4)$$

where:

r, s, t - baricentric coordinates of the element and

$A_{i,j,k}$ - z components of magnetic vector potentials at control points.

The components of the magnetic flux density (5), which we need for the torque calculation (2), can be determined at any point by carrying out the curl operation on (4), since

$$\left.\begin{aligned} B_x &= \left(\frac{\partial A}{\partial r}\frac{\partial r}{\partial y} + \frac{\partial A}{\partial s}\frac{\partial s}{\partial y} + \frac{\partial A}{\partial t}\frac{\partial t}{\partial y}\right) \\ B_y &= -\left(\frac{\partial A}{\partial r}\frac{\partial r}{\partial x} + \frac{\partial A}{\partial s}\frac{\partial s}{\partial x} + \frac{\partial A}{\partial t}\frac{\partial t}{\partial x}\right) \end{aligned}\right\} \Rightarrow B_n, B_t \quad (5)$$

With this we achieved that the calculated components of the magnetic induction in the air gap change continuously and the calculated torque does not depend on discretization.

Algorithm C

In this algorithm the magnetic field in the entire problem domain is calculated by FEM, as in algorithm A or B. Afterwards the air gap region between the rotor and stator is extracted and represents now the Dirichlet's linear problem with known values of the magnetic vector potential on the inner and outer boundary. The field solution by BEM (by mixed boundary elements) gives $\partial A/\partial n$ on both boundaries. The components of the magnetic flux density in this case, can be determined at any point by (6). With this we achieved that the calculated magnetic densities are continuos in the air gap. In the torque calculation (2), as in algorithm C, the number of summands is not conditioned by the number of discretization elements over which the integration path runs. By increasing the number of summands the accuracy of the torque calculation is increased.

$$\left.\begin{aligned} B_x &= \frac{\partial}{\partial y}\left(-\int_l A\frac{\partial G}{\partial n}dl + \int_l G\frac{\partial A}{\partial n}dl\right) \\ B_y &= -\frac{\partial}{\partial x}\left(-\int_l A\frac{\partial G}{\partial n}dl + \int_l G\frac{\partial A}{\partial n}dl\right) \end{aligned}\right\} \Rightarrow B_n, B_t \quad (6)$$

where:

A -boundary values z components of magnetic vector potentials and

G - 2D Green's function .

Algorithm D

The magnetic field is calculated by HM [7], [8]. BEM is used in the air gap between the rotor and stator, and FEM in all other regions. The same characteristics as in algorithm C apply to the solutions in the air gap region.

All algorithms with main steps for torque calculation by MMS are shown in Fig.1.

Calculation of torque		ALGORITHMS			
Step	Calculation	A	B	C	D
1	Field	FEM	FEM	FEM	HM
1+	Recalculation A		Bernst.	BEM	
2	Bn, Bt	(3)	(5)	(6)	(6)
3	Torque	(2)	(2)	(2)	(2)

Fig. 1. Algorithms A, B, C, D.

IV. Numerical Examples

First example

The algorithms were applied and tested in a cogging torque calculation of a permanent magnet DC motor. The discretization of the regions in the motor as used in the FEM and no-load magnetic field for the rotor position of 0 degrees are shown in Fig. 2. The cogging torque was calculated for different choices of the integration path. The integration path radius was changed from the rotor to the stator border (Fig. 3). This calculation was made for the rotor position of four degrees. In this position the cogging torque is maximum.

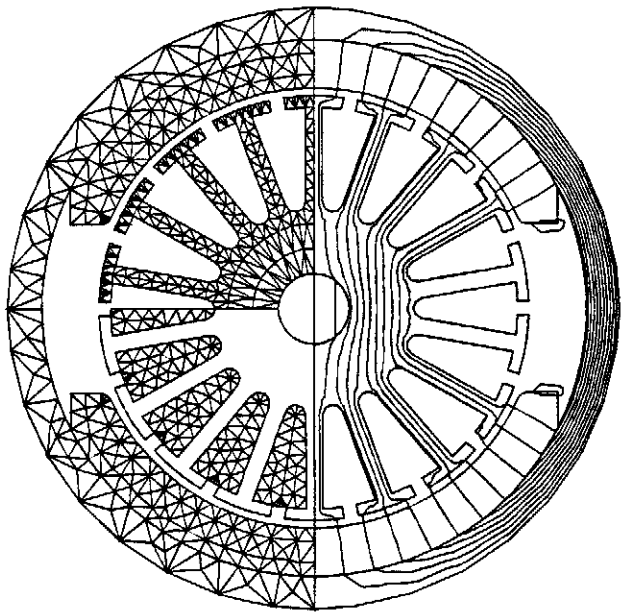

Fig. 2. Mesh and field in the DC PM motor cross-section at 0 degree.

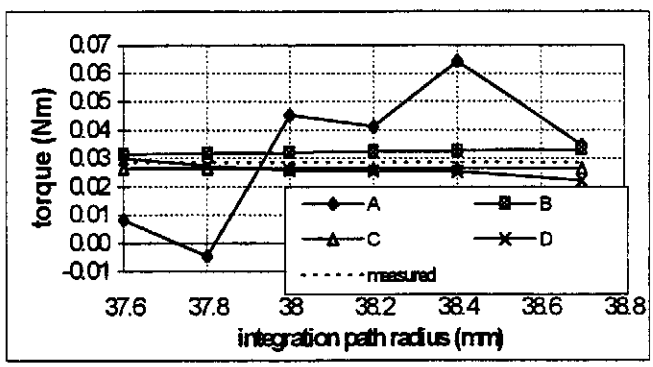

Fig. 3. Influence of the integration path radius on the cogging torque.

TABLE I
INFLUENCE OF THE INTEGRATION PATH RADIUS ON THE COGGING TORQUE.

r (mm)	T by algorithm A (Nm)	T by algorithm B (Nm)
19.02	6.5284766E-02	5.45484E-02
19.04	6.2757313E-02	5.43986E-02
19.08	5.7858620E-02	5.40975E-02
19.12	5.3158958E-02	5.37947E-02
19.16	5.3120464E-02	5.34902E-02
19.20	5.3511206E-02	5.31846E-02
19.22	5.3704765E-02	5.28210E-02
19.24	5.3899023E-02	5.26665E-02
19.26	-0.1214754	5.25117E-02
19.28	2.5657695E-02	5.23564E-02

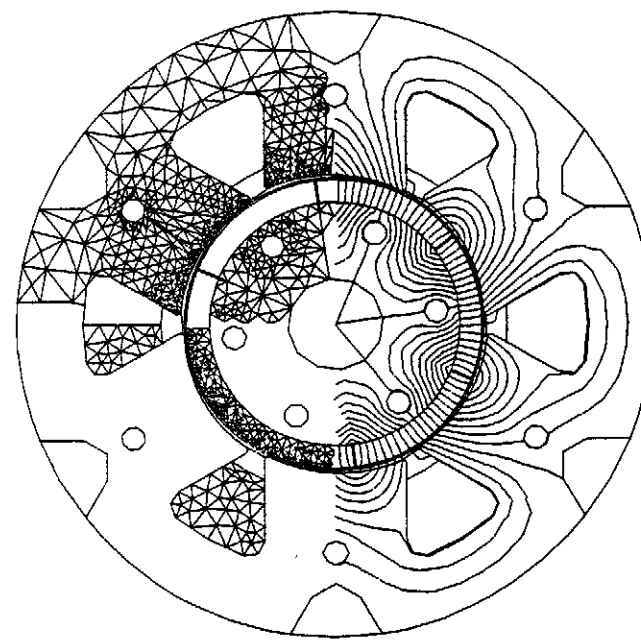

Fig. 4. Mesh and field in the one-phase brushless motor at 30 degree.

SECOND EXAMPLE

A detailed investigation of the cogging torque calculation was performed for a one-phase brushless motor, too (Fig.4). The cogging torque was calculated for different choices of the integration path. The integration path radius has been changed from the rotor to the stator border. The results for different paths of this calculation by the algorithms A and B are shown in Table I. This calculation was made at the 30 degree rotor position. The cogging torque calculation was also made for different rotor positions within one pole division. This division is 60 degrees. In this example the integration path is chosen in the middle of the air gap (r=19.2 mm). In Fig. 5, the results of the cogging torque calculation obtained by the algorithm B together with the measured values are shown. In Fig. 6 , Fig. 7 and Fig. 8, B_n, B_t calculations obtained in the algorithms A, C and D are shown.

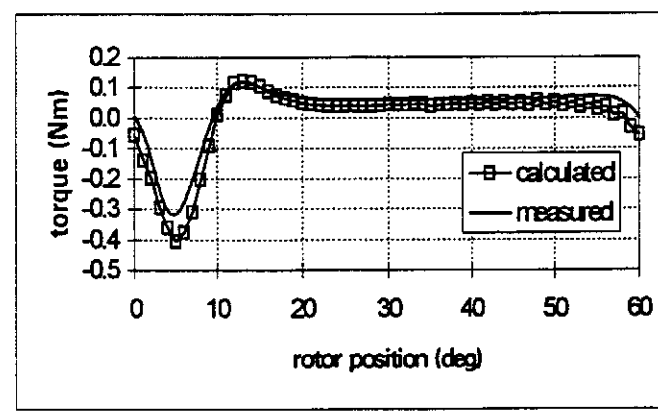

Fig. 5. Cogging torque: calculated by algorithm B and measured values.

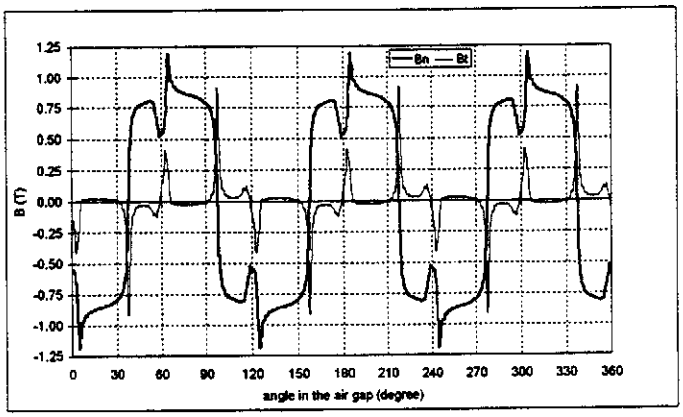

Fig. 6. B_n, B_t calculated in the air gap by FEM.

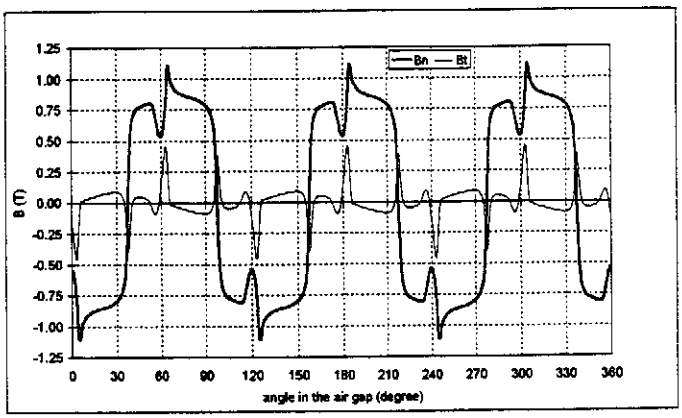

Fig. 7. B_n, B_t calculated in the air gap by BEM (FEM+BEM).

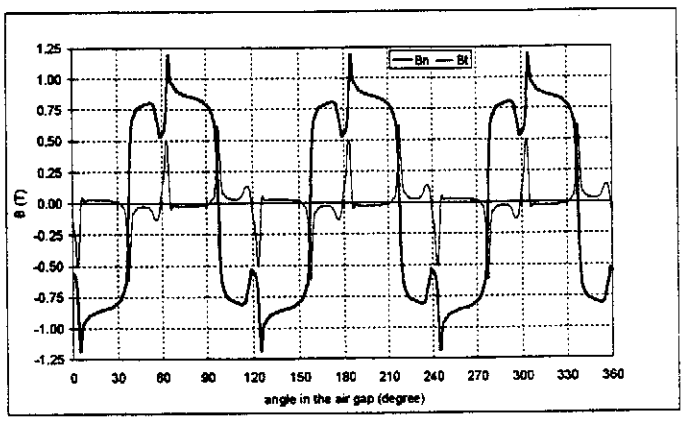

Fig. 8. B_n, B_t calculated in the air gap by HM.

IV. CONCLUSION

In algorithm A the change of the integration path causes large deviations of the calculated torques (Fig. 3, Fig. 5, Table I). In the case of small torques the calculation errors can be up to 100%. In such cases this algorithm is therefore useless.

In algorithms B and C the calculated values of torques are rather independent of the choice of the integration path. Numerically they are favorable, since the magnetic quantities in the air gap are determined in two steps. At first, the field in the entire motor is calculated by FEM and then only the air gap region is treated. The calculated values of magnetic densities are continuos in this area.

Algorithm D is numerically less favorable since HM is used. The use of BEM in the air gap region results in a nonsymmetric system matrix. The advantage of the algorithm is the possibility to release the connections between the rotor and stator, which is favorable if the rotor position is changing in the torque calculation.

REFERENCES

[1] P.P. Silvester, R.L. Ferrari, Finite Element for Electric Engineers, Cambridge University Press, Cambridge, 1987.

[2] Y.G. Park, H. Kim and S. Hahn: "An Adaptive Finite Element Method for Magnetostatic Force Computations." *IEEE Trans. Mag.*, Vol. 26, No. 2, pp. 1031-1034, March 1990.

[3] P. A. Watterson: "Torque Evaluation for 2-D Finite Element Field Solutions." *Compumag 91*, July 7-11, pp. 767-770, 1991 - Sorrento, Italy.

[4] G. Farin, "Triangular Bernstein-Bézier patches." *Computer Aided Geometric Design* 3(2), pp. 83-128. 1986.

[5] A. Hamler, B. Hribernik, M. Likar, N. Guid, Torque Calculation by Bernstein Bézier's Surfaces, IEEE Transaction on Magnetics, vol. 31, no. 3, pp. 1885-1887, May 1995.

[6] C. A. Brebbia, Topics in Boundary Element Research, Volume 6, Electromagnetic Applications, Springer-Verlag Berlin Heidelberg, 1989.

[7] S.J. Salon., The Hybrid Finite Element - Boundary Element Method in Electromagnetics, IEEE Transactions on Magnetics, Vol. MAG-21, No.5, pp.1040-1042, 1985.

[8] M. Trlep, P. Škerget, B. Kreča, B. Hribernik, Hybrid Finite Element-Boundary Element Method for Nonlinear Electromagnetic Problems, IEEE Transactions on Magnetics, vol. 31, no. 3, pp. 1380-1383, May 1995.

[9] M. Jesenik, M. Trlep, B. Hribernik, Automatic 2D Discretization with Variable Mesh Density for Numerical Methods, V: Electric and Magnetic Fields, New York, London: Plenum Press, pp. 181-184, 1995.